Theoretical and Applied Climatology (2026) 157:373
https://doi.org/10.1007/s00704-026-06305-9

RESEARCH

The Saharan oscillation index (1950–2024): phase structure, regime shifts, and global teleconnections

Younes Tebbaai[1,2] · Kenza Khomsi[2] · Mohamed Khalis[1,3]

Received: 9 February 2026 / Accepted: 5 May 2026
© The Author(s), under exclusive licence to Springer-Verlag GmbH Austria, part of Springer Nature 2026

Abstract

The Saharan Oscillation Index (SaOI) quantifies the pressure gradient between the Azores High and the Saharan low centered near Niamey, capturing atmospheric variability that influences climate across the Euro-Atlantic-African region. Despite its importance for regional hydroclimate, dust transport, and air quality, its phase behavior and teleconnections with global climate modes remain insufficiently characterized. Here, we analyze 75 years (1950–2024) of SaOI variability using standardized phase classification and seasonal lag-correlation analysis with thirteen large-scale climate indicators (LSCIs). The SaOI exhibits three distinct periods: a balanced phase distribution (1950–1965), sustained variability (1965–1990), and a pronounced shift toward positive-neutral dominance after 1990, with a marked decline in negative phase frequency after 2010. The SaOI shows moderate but statistically significant correlations with the North Atlantic Oscillation Index (NAOI; r=0.42, 95% CI [0.21, 0.59]), Arctic Oscillation Index (AOI; r=0.42, 95% CI [0.21, 0.59]), and Oceanic Niño Index (ONI; r = -0.44, 95% CI [-0.61, -0.24]). These relationships explain approximately 18–19% of the interannual variance, indicating meaningful but not strong coupling within a multifactorial climate system. Seasonal analysis further reveals lagged teleconnections extending from late winter through summer, highlighting the combined influence of extratropical and tropical processes on Saharan circulation. Positive SaOI phases are associated with enhanced pressure gradients that strengthen trade winds, suppress precipitation, and increase dust activity, whereas negative phases promote moisture advection and convective activity. The apparent regime shift after 1990 suggests potential non-stationarity, possibly driven by anthropogenic forcing and/or natural multidecadal variability, although formal change-point verification using non-parametric methods is beyond the scope of this study. These findings establish the SaOI as a useful diagnostic tool for subseasonal-to-seasonal prediction, with direct applications in drought early warning, dust storm forecasting, and heat-risk preparedness across the Sahel, Maghreb, and Mediterranean regions.

Abbreviations

SaOI	Saharan Oscillation Index
LSCIs	Large-Scale Climate Indicators
NAOI	North Atlantic Oscillation Index
AOI	Arctic Oscillation Index
ONI	Oceanic Niño Index
SOI	Southern Oscillation Index
MOI	Mediterranean Oscillation Index
TNAI	Tropical Northern Atlantic Index
TSAI	Tropical Southern Atlantic Index
WHPI	Western Hemisphere Warm Pool Index
PDOI	Pacific Decadal Oscillation Index
PNAI	Pacific North American Index
NPI	North Pacific Index
NOI	Northern Oscillation Index
WPI	Western Pacific Index
SST	Sea Surface Temperature
SLP	Sea Level Pressure
Z500	Geopotential Height at 500 hPa
ERA5	ECMWF Reanalysis v5
CRU	Climatic Research Unit
AOD	Aerosol Optical Depth

✉ Younes Tebbaai
ytebbaai@um6ss.ma

[1] Department of Public Health and Clinical Research, Mohammed VI Center for Research and Innovation, Rabat, Morocco

[2] Mohammed VI International School of Public Health, University of Sciences and Health, Mohammed, Casablanca, VI, Morocco

[3] Higher Institute of Nursing Professions and Health Techniques, Ministry of Health and Social Protection, Rabat, Morocco

Published online: 15 May 2026

S2S	Subseasonal-to-Seasonal
AMV	Atlantic Multidecadal Variability
SAM	Southern Annular Mode

Climatological Seasons

DJF	December - January - February
JFM	January - February - March
FMA	February - March - April
MAM	March - April - May
AMJ	April - May - June
MJJ	May - June - July
JJA	June - July - August
JAS	July - August - September
ASO	August - September - October
SON	September - October - November
OND	October - November - December
NDJ	November - December - January

1 Introduction

The Sahara is one of the most climatically influential regions on Earth, exerting a far-reaching impact on atmospheric circulation, surface energy balance, and global dust transport. Its intense land-atmosphere coupling and large thermal gradients modulate the West African Monsoon system, the Mediterranean climate, and even remote teleconnections across the Atlantic and Pacific basins (Giannini et al. 2003; Nicholson 2013; Rodríguez-Fonseca et al., 2016). Fluctuations in the Saharan pressure system control large-scale subsidence, humidity transport, and dust emission processes that strongly affect temperature, precipitation, and air quality across North Africa and adjacent regions (Goudie and Middleton 2001; Lelieveld et al. 2015; Prospero et al. 2002). These dynamics are coupled to regional hydrological and health outcomes through recurring droughts, extreme heat events, and particulate matter exposure (Cramer et al. 2018; Dosio et al. 2019; Tanarhte et al. 2024).

Despite this central climatic role, the Saharan atmospheric circulation had long lacked a specific diagnostic index capable of capturing its interannual and multidecadal variability. To address this gap, Khomsi et al. 2020 introduced the (SaOI), a physically based measure of the pressure gradient between the Azores High and the Saharan thermal low. The SaOI provides a simple yet robust descriptor of Saharan atmospheric dynamics, analogous to other global indices such as the NAO (Hurrell 1995; López-Moreno and Vicente-Serrano 2008), the AO (Thompson and Wallace 2001; Zhang et al., 2021), and the PDO (Frankcombe et al. 2010; Mantua et al. 1997). However, the SaOI uniquely represents the dynamics of the Saharan region, an area previously underrepresented in the global teleconnection framework by linking large-scale pressure anomalies to local and regional climatic variability.

While the Azores High and Saharan Thermal Low are well-established as individual centers of action, a dedicated multi-decadal analysis of their coupled variability via the SaOI spanning 1950–2024 is necessary to establish the index's statistical characteristics. Preliminary observations suggest the existence of distinct climatic epochs and potential regime shifts in the region after the early 1990s. However, the internal phase structure of the SaOI, representing alternating positive, negative, and neutral circulation regimes, has not yet been systematically classified. Furthermore, the teleconnections between SaOI and other LSCIs remain unquantified. Understanding these relationships is essential for situating the SaOI within the global climate system and clarifying how Saharan circulation interacts with dominant modes such as the NAO, AO, PDO, and El Niño-Southern Oscillation (ENSO) (Barnston and Livezey 1987; Wallace & Gutzler, 1981; Rodríguez-Fonseca et al., 2016; Sultan and Gaetani 2016). These teleconnections can shape regional hydrological variability, dust activity, and temperature anomalies across the Sahel-Mediterranean corridor (Bouguerra et al. 2024; Hurrell 1995; Lavaysse et al. 2018).

The present study addresses these gaps by systematically investigating the phase behavior and global teleconnections of the SaOI over 1950–2024. Specifically, it addresses three unresolved questions: (a) how SaOI phases are distributed across multi-decadal timescales, (b) how the SaOI is linked to a broader suite of large-scale climate indicators, and (c) whether its long-term behavior suggests a potential regime shift. To address these questions, we classify SaOI phases using a standardized threshold approach and examine their relationships with thirteen LSCIs representing major atmospheric and oceanic modes across the Northern Hemisphere and tropics. Through this framework, the study aims to clarify the place of the SaOI within the broader teleconnection network and to identify the main physical links connecting Saharan circulation with remote climate drivers.

The originality of this work lies in combining dynamical phase classification with global correlation analysis to better situate the SaOI within the planetary circulation framework. This approach improves understanding of how Saharan circulation variability is linked to hydroclimate, drought persistence, and dust transport, all of which have strong environmental and socio-economic relevance. The remainder of the paper is organized as follows: Sect. 2 describes the data and methods, Sect. 3 presents the results, Sect. 4 discusses their climatic interpretation, and Sect. 5 concludes with implications for climate monitoring and risk assessment.

2 Scale climate in

This study investigates the (SaOI) through two complementary approaches: (1) phase classification to identify distinct circulation regimes, and (2) seasonal lag-correlation analysis to quantify teleconnections with LSCIs. The phase classification provides the foundation for understanding SaOI temporal variability and potential regime shifts, while the correlation approach reveals its physical coupling with global climate modes.

2.1 Large-Scale Climate Indicators (LSCIs)

We assessed annual and seasonal relationships between the SaOI and thirteen LSCIs spanning 1950–2024. The selection of these indicators was based on the comprehensive review by Khomsi et al. (2024), prioritizing modes with established teleconnections to the Mediterranean and North African hydroclimate to ensure regional relevance (Criado-Aldeanueva & Soto-Navarro, 2020; Khomsi et al., 2024). The dataset includes atmospheric and oceanic indices sourced from the NOAA Physical Sciences Laboratory and the Climatic Research Unit (CRU). All indices were analyzed in their standardized anomaly form as supplied by the respective data sources, and no additional detrending was applied. The rationale for selecting these thirteen indices is summarized in Table 1, while detailed technical definitions, data sources (Bouguerra et al. 2024; Hurrell 1995; J. Li & Wang, 2003), and known Mediterranean impacts are presented in Supplementary Table S1. Detailed statistical diagnostics, including raw correlation coefficients, p-values, and effective degrees of freedom (Neff), are reported in Supplementary Figure S1.

2.2 Definition of the Saharan oscillation index (SaOI)

The SaOI is defined as the standardized pressure difference between the Azores High and the Saharan Niamey Low (Khomsi et al. 2020). Using monthly mean sea level

Table 1 Summary of used LSCIs and their selection justification

Category	Climate Indicator	Selection Justification
Extratropical Atmospheric	North Atlantic Oscillation (NAOI)	Primary driver of North Atlantic atmospheric mass; controls Mediterranean moisture transport (Hurrell 1995; Luppichini et al. 2024).
	Mediterranean Oscillation (MOI)	Captures regional dipole oscillations essential for western vs. eastern Mediterranean hydroclimate (Bouguerra et al. 2024; Palutikof 2003).
	Arctic Oscillation (AOI)	Reflects polar vortex intensity; modulates mid-latitude westerlies affecting North African pressure (Fang et al. 2024).
	Northern Oscillation (NOI)	Linked to North Pacific SLP fluctuations and broader hemispheric atmospheric dynamics (Schwing et al. 2002).
	Western Pacific Index (WPI)	Affects planetary wave propagation and changes in global atmospheric circulation (Aru et al. 2021; Zhuge & Tan, 2018, 2021.
	Pacific North American (PNAI)	Winter-dominant pattern affecting the jet stream and downstream North Atlantic circulation (Hu et al. 2023; Wallace & Gutzler, 1981).
	North Pacific Index (NPI)	Measures Aleutian Low intensity, modulating westerly flow toward the Mediterranean (Minobe and Mantua 1999; Xiao and Ren 2023).
Tropical Oceanic	Oceanic Niño Index (ONI)	Main metric for ENSO; directly impacts Mediterranean autumn and spring rainfall regimes (Glantz and Ramirez 2020; Vimont et al., 2022).
	Southern Oscillation (SOI)	Atmospheric component of ENSO; linked to temperature and rainfall fluctuations in the western Mediterranean (Clement et al. 2011; Power and Kociuba 2011).
	Tropical Northern Atlantic (TNAI)	Critical for monitoring SST anomalies that influence Saharan dust transport and regional weather (Chen & Wu, 2017).
	Tropical Southern Atlantic (TSAI)	Part of the Atlantic dipole modulates the West African Monsoon and regional thermal gradients (Sheng et al. 2023; Yang and Fan 2023).
	Western Hemisphere Warm Pool (WHPI)	Affects Hadley/Walker cell dynamics, influencing Mediterranean weather during pool expansion (Enfield et al. 2006; López-Magaña et al. 2022; Park et al. 2018; Wang and Enfield 2001).
Multidecadal Modes	Pacific Decadal Oscillation (PDOI)	Modulates interannual climate patterns and Mediterranean precipitation over decadal scales (Boer and Sospedra-Alfonso 2019; Deser et al. 2016; Li et al. 2015).

pressure (SLP) derived from daily ERA5 reanalysis data at 0.25° spatial resolution (Hersbach et al., 2020) (1950–2024), we extracted pressure series at the climatological centers illustrated in Fig. 1: Ponta Delgada, Azores (37.79°N, 25.5°W) and Niamey, Niger (13.51°N, 2.10°E). Daily values were used to compute monthly means, ensuring that high-frequency variability was captured before averaging. Because ERA5 is a quality-controlled reanalysis product, no additional station-level homogenization was required. The extracted sea level pressure series were nevertheless checked for completeness prior to analysis, and no substantial data gaps were identified.

The daily SaOI ($SaOI_d$) is calculated as:

$$SaOI_d = P^*_{Azores} - P^*_{Niamey}$$

2.3 Methods

2.3.1 The SaOI phase classification

The SaOI phase classification employs a standardized ±1σ threshold method, a robust approach widely used for major climate indicators, including the NAO (Hurrell 1995; Jones et al. 1997; J. Li &Wang, 2003), Pacific Decadal Oscillation (Mantua et al. 1997), and El Niño-Southern Oscillation (Trenberth 1997).

Monthly SaOI values were classified into three phases using deviations from the long-term mean ($\mu = 0.20$) relative to the standard deviation ($\sigma = 0.11$) calculated over the entire 1950–2024 period. Although the SaOI distribution exhibits slight positive asymmetry, the ±1σ threshold was retained to ensure consistency with widely used climate-index classification frameworks. This approach is therefore applied as a pragmatic classification method rather than a strict assumption of normality. This classification scheme, consistent with methodologies applied to the NAO (Hurrell and Deser 2009) and PDO (Mantua et al. 1997), theoretically assigns approximately 68% of observations to the neutral category and 16% each to positive and negative phases under normal distribution assumptions. The standard deviation-based approach accounts for natural variability while providing reproducible phase assignments for composite analysis and climate impact assessment (Gershunov and Barnett 1998; Pokorná and Huth 2015). The phases are defined as:

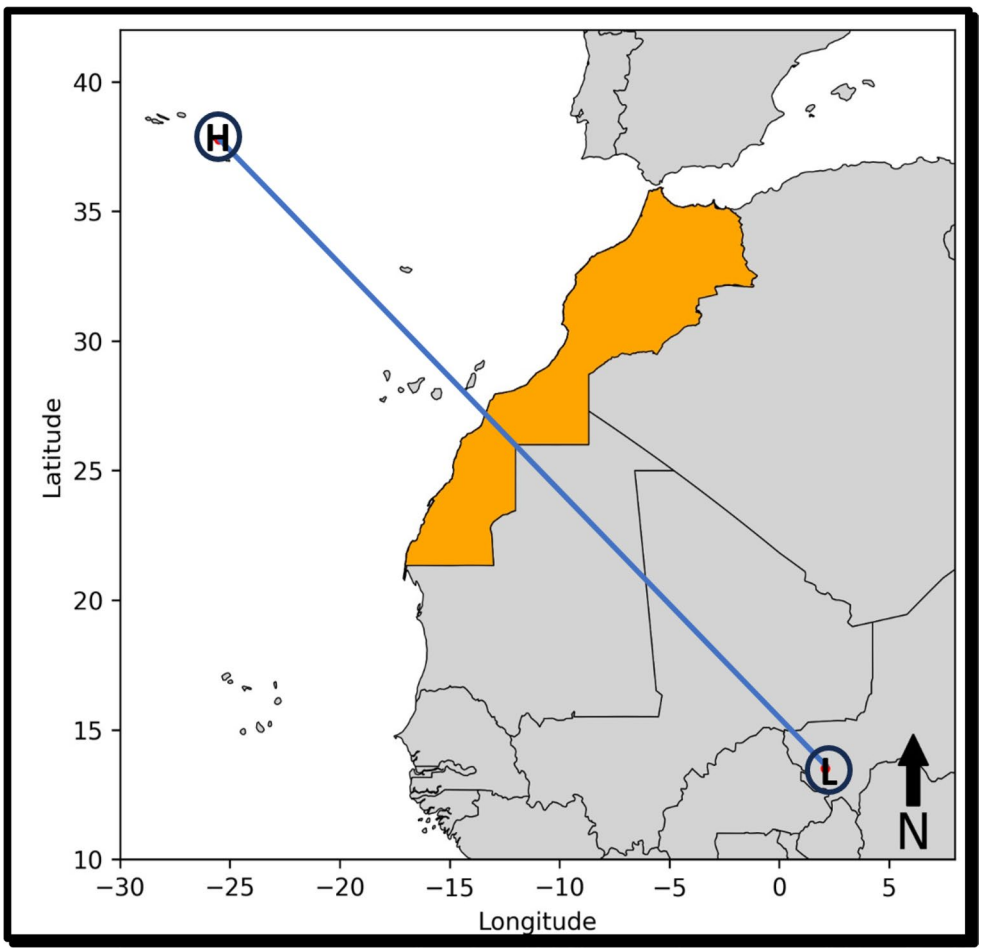


Fig. 1 Geographic locations of the Azores High (H) and Saharan Low (L) used to compute the SaOI. The Azores High point is at Ponta Delgada (37.79°N, 25.5°W), and the Saharan Low point is at Niamey, Niger (13.51°N, 2.10°E)

- Positive Phase: $SaOI > \mu + \sigma$
- Negative Phase: $SaOI < \mu - \sigma$
- Neutral Phase: $\mu - \sigma \leq SaOI \leq \mu + \sigma$

2.3.2 Seasonal lag-correlation and significance testing

Seasonal and interannual teleconnections between the SaOI and thirteen LSCIs were examined using a seasonal lag-correlation framework. This method is widely applied in atmospheric teleconnection studies to identify both simultaneous (lag-0) and lead-lag relationships (Wallace & Gutzler, 1981; Thompson & Wallace, 1998).

Twelve overlapping 3-month seasons were defined (NDJ, DJF, JFM, FMA, MAM, AMJ, MJJ, JJA, JAS, ASO, SON, OND), following Hurrell et al. (2003). Overlapping seasons help reduce high-frequency noise and capture the gradual evolution of SaOI-related variability across the annual cycle (Nicholson 2013). Seasonal means ($\bar{X}_s$) were calculated as:

$$\bar{X}_s = \frac{1}{3}\sum_{m \in s} X_m$$

where X_m are the months in season s and year assignment follows the convention of using the year containing January (Barnston and Livezey 1987). For each pair of indices, the Pearson correlation coefficient (r) was computed to assess the relationship between the SaOI (X) and the target LSCI (Y):

$$r = \frac{\sum_{i=1}^{n}\left(X_i - \bar{X}\right)\left(Y_i - \bar{Y}\right)}{\sqrt{\sum_{i=1}^{n}\left(X_i - \bar{X}\right)^2 \sum_{i=1}^{n}\left(Y_i - \bar{Y}\right)^2}}$$

To ensure the statistical markers are robust against Type I errors arising from multiple hypothesis testing (168 correlation pairs), a False Discovery Rate (FDR) adjustment was applied to the p-values following the Benjamini-Hochberg procedure (Benjamini and Hochberg 1995). The FDR procedure identifies significant correlations by ranking m p-values $\left(p_{(1)} \leq p_{(2)} \leq \ldots \leq p_{(m)}\right)$ and satisfying the condition:

$$p_{(k)} \leq \frac{k}{m}$$

where $\alpha = 0.05$. Furthermore, because overlapping seasons introduce artificial persistence, the significance testing was adjusted using the effective degrees of freedom (N_{eff}) to account for serial correlation (Pyper and Peterman 1998; Santer et al. 2000).

The t-statistic for each correlation was calculated as:

$$t = r\sqrt{\frac{N_{eff} - 2}{1 - r^2}}$$

Where $(\mathrm{N_{eff}})$ was estimated as:

$$N_{eff} \approx N\frac{1 - \rho_1\rho_2}{1 + \rho_1\rho_2}$$

In this formulation ρ_1 and ρ_2 are the lag-1 autocorrelation coefficients of the two-time series. Significant correlations $p_{FDR} < 0.05$ are visualized using a diverging Red-Blue colormap.

3 Results and discussion

3.1 SaOI phase characteristics and long-term variability (1950–2024)

3.1.1 Variability structure and phase asymmetry

The SaOI exhibits a range of approximately 0.75 units over the 1950–2024 period, with a mean (μ) of 0.1954 and a standard deviation (σ) of 0.1137. As illustrated in Fig. 2, this distribution defines phase thresholds of 0.31 for the positive phase and 0.08 for the negative phase. The positive mean suggests a tendency toward enhanced North Atlantic subtropical high-pressure influence (Azores High). While neutral conditions dominate the record, positive phases are more frequent and intense than negative phases, indicating an asymmetry in the circulation's variability. This asymmetry implies that extreme positive phases may exert a disproportionate influence on regional precipitation and temperature patterns across North Africa and the Mediterranean.

3.2 Temporal evolution and potential regime change

Three distinct epochs emerge from the record. The early period (1950–1965) exhibits a balanced phase distribution, with the most pronounced negative events approaching −0.20 in the early 1960s. The intermediate period (1965–1990) maintains strong variability, with notable clustering of negative phases during the 1960 s and 1980 s, coinciding with documented Pacific-Atlantic interactions (Rodríguez-Fonseca et al. 2009).

The most prominent feature occurs after 1990, with a marked reduction in both the frequency and intensity of negative phases and a transition toward positive–neutral dominance, which intensifies after 2010. The 2003–2005 period shows exceptional positive anomalies exceeding 0.45. This shift is consistent with documented hydroclimatic

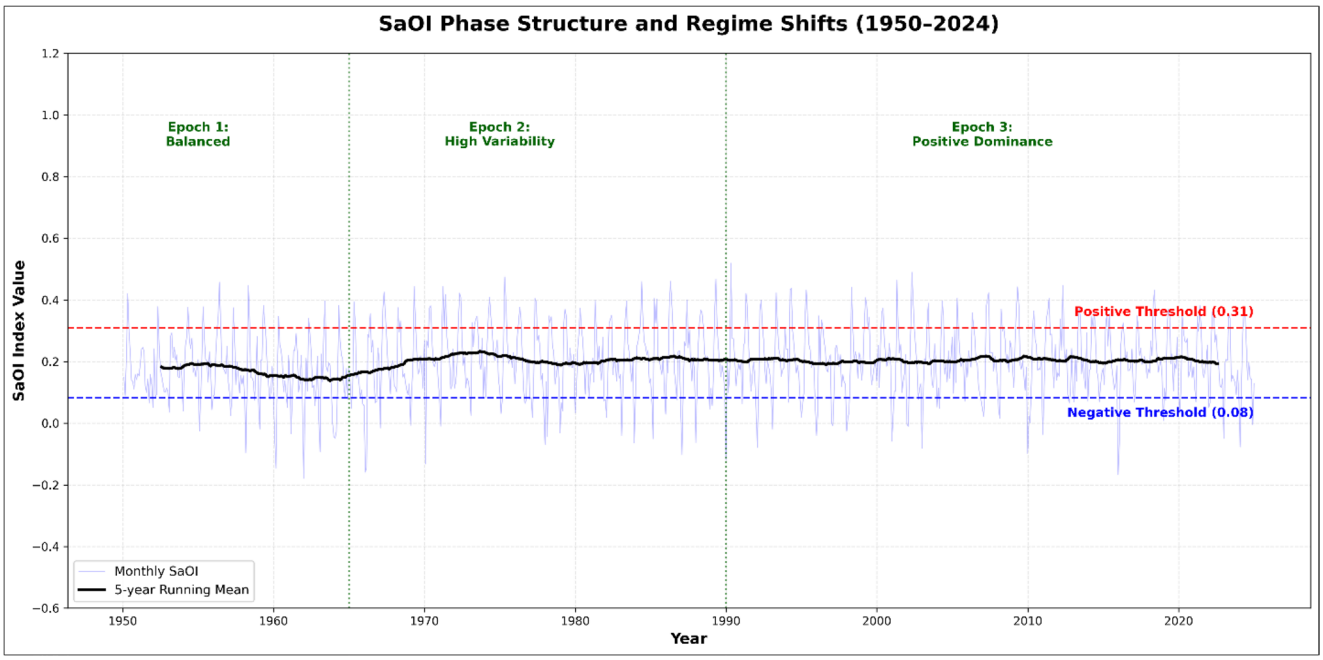


Fig. 2 Temporal evolution and phase classification of the SaOI (1950–2024). The monthly SaOI is shown as a light blue line, while the 5-year running mean (solid black line) highlights low-frequency variability and regime shifts. Horizontal dashed lines indicate the phase thresholds derived from the long-term mean ($\mu = 0.20$) and standard deviation ($\sigma = 0.11$), corresponding to the positive phase (red; $SaOI \geq \mu + \sigma \approx 0.31$) and negative phase (blue; $SaOI \leq \mu - \sigma \approx 0.08$). Vertical dotted lines mark the boundaries between the three identified epochs (1965 and 1990), illustrating the transition toward a positive-dominated regime in recent decades

changes in Morocco around 1990, where regional precipitation and temperature patterns underwent a structural transition toward warmer and drier conditions (Sebbar et al. 2011; Verner et al. 2018). This post-2010 intensification may be further influenced by the documented 2013/14 Pacific climate regime shift, which has been shown to alter global teleconnection patterns and atmospheric circulation (Meehl et al. 2016). This apparent regime shift raises critical questions about underlying drivers, whether anthropogenic forcing on the Hadley Cell (Frierson et al. 2007b), natural multidecadal variability linked to the Atlantic Multidecadal Variability (AMV) (Enfield et al. 2001), or altered teleconnections with ENSO and the Southern Annular Mode (Fogt and Marshall 2020).

While these observations of a structural transition are striking, they remain primarily qualitative in the current study. Consequently, formal statistical verification via change-point detection tests (Lee and Heghinian 1977; Pettitt 1979) is required to confirm a definitive regime break.

3.3 Physical mechanisms and predictability

Phase persistence, evidenced by the clustering of consecutive monthly anomalies, indicates significant atmospheric memory. This persistence is quantitatively supported by a significant positive lag-1 autocorrelation of the SaOI ($\rho_1 \approx 0.50$), confirming pronounced temporal dependence in the monthly index and reinforcing the need to account for serial correlation through effective degrees of freedom (Neff) in significance testing. Such memory is likely maintained through coupled feedback mechanisms. Positive phases are characterized by an intensification of the North Atlantic subtropical high (Azores High), which strengthens the trade wind inversion and modulates moisture convergence zones essential for North African precipitation (Davis et al. 1997; Hurrell and Deser 2009). Conversely, negative phases reflect a weakening of these pressure gradients, disrupting canonical circulation and displacing mid-latitude storm tracks. The dominance of the neutral phase suggests that the system spends substantial time in transitional states that are highly sensitive to external stochastic forcing.

The recent shift toward a positive–neutral regime has important implications for seasonal forecasting and water resource management in the Mediterranean, particularly in regions that have historically adapted to more variable circulation conditions (Sebbar et al. 2011). This transition may reflect a non-stationary response to global warming (Frierson et al., 2007) or multidecadal variability linked to the Atlantic Multidecadal Variability (Enfield et al. 2001). Understanding the mechanisms driving this shift is essential for improving subseasonal-to-seasonal (S2S) predictability (Vitart et al. 2017).

3.4 Links between SaOI and other LSCIs

3.4.1 Annual and seasonal correlations with LSCIs

Before presenting the correlation outcomes, it is important to clarify that all statistically significant relationships identified between the SaOI and other LSCIs were of moderate strength, with the Pearson correlation coefficients generally falling within the range of $0.40 \leq |r| \leq 0.57$. No strong correlations were observed, which reflects the multifactorial and complex nature of atmospheric teleconnections governing Sahel-Mediterranean climate dynamics.

On an annual basis, the SaOI exhibited consistent, statistically significant associations $(p < 0.05)$ with three primary (centers of action): the NAOI, AOI, and ONI (Fig. 3). These three indicators represent the dominant perennial drivers of Saharan atmospheric variability, satisfying the dual criteria of moderate coupling $(|r| \geq 0.40)$ and statistical significance after accounting for serial correlation.

While seasonal analyses show further moderate correlations for these indices, they also reveal significant lagged seasonal correlations with tropical Atlantic modes (TNAI and TSAI), despite their non-significant associations on an annual mean basis. This divergence stresses that while the North Atlantic and Pacific exert year-round influence, other tropical climate drivers act as seasonally dependent modulators throughout the annual cycle.

3.4.2 SaOI and NAOI

According to (Fig. 3), the annual correlation between SaOI and NAOI is 0.42. This indicates a moderate statistical association between the Saharan and North Atlantic pressure systems, thereby depicting the sway NAO variability casts on Saharan atmospheric phenomena.

Seasonal variations provide deeper insight into this relationship, as illustrated in (Fig. 4). During NDJ, the SaOI shows moderate positive correlations with NAOI (0.52) and DJF (0.42), suggesting simultaneous and slightly lagged coupling of the two indices towards the onset of winter. This relationship carries through to (DJF), where SaOI continues to be related to NAOI in NDJ (0.49) and DJF (0.58), supporting a consistent mid-winter teleconnection.

In late winter, the NAO influence extending into Saharan pressure variability is pronounced, with sustained seasonal correlations between NAOI and the southern pressure system from late autumn to spring. More specifically, the averaged SaOI from January to March continues to exhibit a significant positive correlation with NAOI in NDJ (0.44), DJF (0.57), JFM (0.56), and FMA (0.41). This relationship further persists into FMA, where SaOI remains positively and significantly correlated with NAOI in DJF (0.49), JFM (0.53), and FMA (0.48), indicating a prolonged seasonal coupling.

In fact, these cases indicate that the influence is maintained late into winter and extends well into early spring. On the other hand, in MAM, the SaOI is also positively linked to NAOI in MAM (0.47), thereby implying that such linkages remain late into the cold season, yet, no lagged correlations appear. These correlations seem to provide strong evidence supporting the hypothesis that the Saharan pressure system is modulated by NAO in particular from late autumn to early spring.

These atmospheric interactions may bear environmental, public health, and many other implications. For instance, the positive phase of the NAO associated with intensification of the Azores High would intensify subsidence and dryness over North Africa. This contributes to drought development particularly when coupled with a positive SaOI, which lures the Saharan thermal low and cuts convective precipitation. Such a combination of conditions causes a delay in or a weakening of West African Monsoon onset to the negative impact on agricultural productivity and food security, particularly in the Sahel and Maghreb(Giannini et al. 2003; Mazouz et al. 2013; Nicholson 2013).

The spring activity of the SaOI assists in early-season heatwave formation, although the SaOI is inactive in

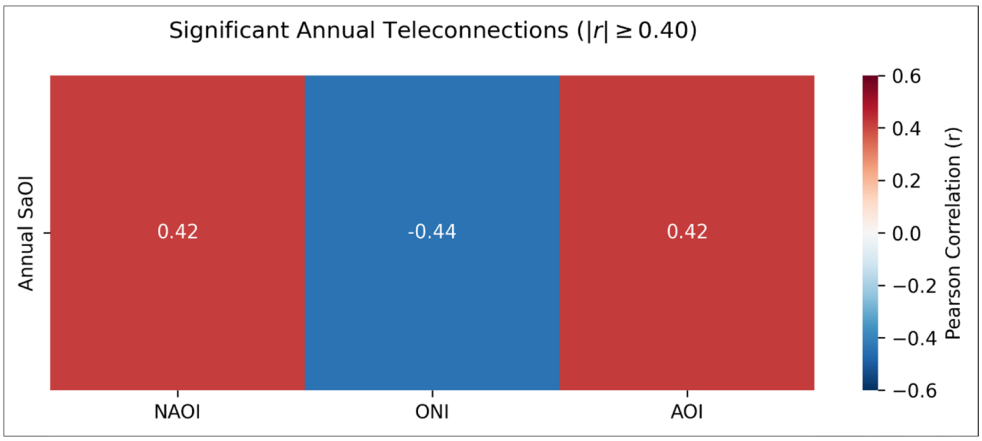


Fig. 3 Annual teleconnections between the SaOI and robust LSCIs (1950–2024). Only correlations meeting both the strength criterion ($|r| \geq 0.40$) and statistical significance (FDR-adjusted p-value < 0.05, accounting for effective degrees of freedom, N_{eff}) are shown

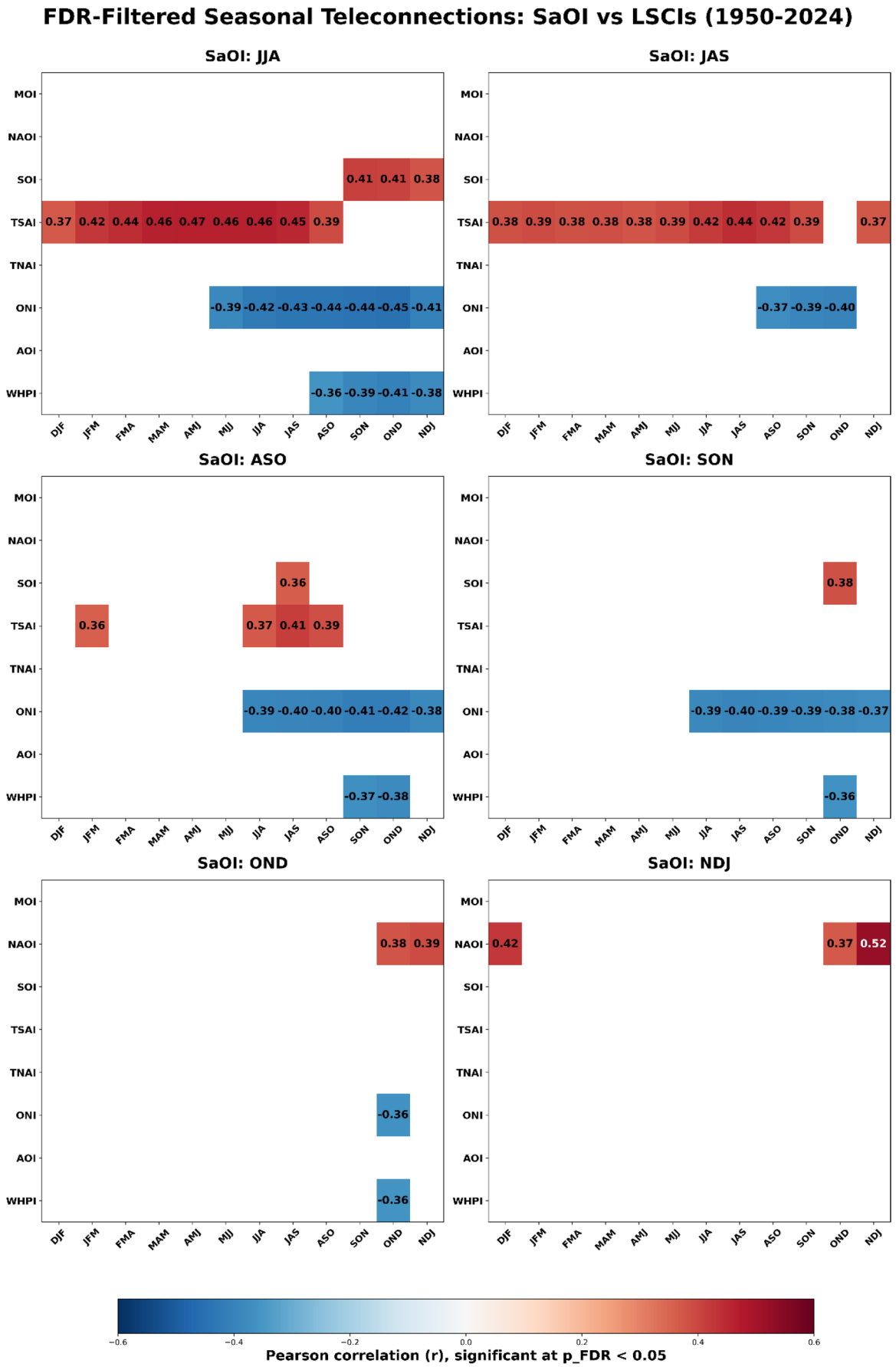

FDR-Filtered Seasonal Teleconnections: SaOI vs LSCIs (1950-2024)
SaOI: JJA
SaOI: JAS
SaOI: ASO
SaOI: SON
SaOI: OND
SaOI: NDJ
MOI
NAOI
SOI
TSAI
TNAI
ONI
AOI
WHPI
DJF JFM FMA MAM AMJ MJJ JJA JAS ASO SON OND NDJ
Pearson correlation (r), significant at p_FDR < 0.05

Fig. 4 Seasonal teleconnections between the (SaOI) and significant LSCIs for the period 1950–2024. Panels represent the Pearson correlation coefficients (r) for twelve overlapping seasons of the SaOI: **(a)** phases DJF through MJJ and **(b)** phases JJA through NDJ. Only correlations satisfying the Benjamini-Hochberg False Discovery Rate (FDR) adjustment ($p_{FDR} < 0.05$) are displayed with numerical values and color. Red and blue shades indicate positive and negative associations, respectively

summer. During those strong positive SaOI phases, especially when coupled with a persistent positive NAO, the Saharan Low deepens, promoting insolation and discouraging convective cooling. Thermal anomalies bring about heat accumulation at the surface across the Sahara, the Sahel, and the Mediterranean fringe, adding to these spring heatwaves, which intensify hydric stress, diminish soil moisture, and threaten water availability(Cramer et al. 2018; Dosio et al. 2019; Lavaysse et al. 2018).

Lastly, the coupling further fosters dust activity. The increased pressure gradient during positive phases of SaOI also increase the wind field, thereby mobilizing Saharan dust from source regions such as the Bodélé Depression and Tamanrasset Basin. These plumes then cross the Mediterranean and Atlantic into the downwind areas, compromising air quality and thereby exacerbating health risks, especially for respiratory and cardiovascular conditions(Lelieveld et al. 2013, 2015; Prospero et al. 2002).

3.4.3 SaOI and AOI

Although the annual correlation between the SaOI and AOI (Fig. 3) is significant ($r = 0.42$), this relationship differs from the SaOI-NAOI link in that it remains statistically insignificant throughout much of the year; therefore, one cannot imply that these indices interact persistently. Only moderate positive correlations appear around late winter to early spring (Fig. 4).

The SaOI during JFM is found to be significantly positively correlated with AOI in DJF (0.42) and JFM (0.41), implicating some atmospheric variability at high latitudes, such as the strength of the polar vortex and modulates mid-latitude westerlies and associated Rossby wave propagation, affecting North African pressure gradients, in the modulation of the Saharan pressure systems during late winter. This link is intensified in FMA, wherein SaOI correlates positively with AOI in DJF (0.43) and JFM (0.44). In MAM, correlation further sustains with the AOI of the same period (0.43). Furthermore, a significant linkage is recorded in the period AMJ, wherein the SaOI bears a positive correlation with AOI (0.45), furthering the late-spring influence of polar dynamics.

This teleconnection would permit enhanced westerlies to translate downward and equatorward along with the polar vortex strength, constituted by the positive AO phase, shaping subtropical pressure gradients over North Africa. Such behavior is likely to increase the Saharan Low through intense subsidence, which delays rainfall onset and increases drought risk across the Maghreb and Sahel lands (Paz et al. 2003; Thompson and Wallace 2001; Tourre et al. 2006).

Nevertheless, the positive springtime coupling between SaOI and AOI can favor an early-season onset of heatwaves. Strong positive phases of AO force subsidence and clear-sky conditions, which maximize thermal influence over North Africa and Southern Europe, particularly when acting in synergy with a positive SaOI. These spring heatwaves would boost evapotranspiration, thereby deepening soil dryness and alarming both water resources and the public health systems (Dosio et al. 2020; Lavaysse et al. 2018; Perkins-Kirkpatrick and Lewis 2020).

Dust activity, with respect to the SaOI-AOI relationship, offers only a background conducive atmospheric situation because unless particular phenomena are triggered, the onset of a dust storm cannot be directly attributed to this relationship. Though it is spring, high-pressure gradients along with dry soil moisture profiles namely, from AOI-induced subsidence, act in synergy to uproot and carry dust-driven phenomena, which seriously aggravate air pollution and elevate associated health risks, especially those related to respiratory and cardiovascular endpoints (Middleton 1985; Pu and Ginoux 2017).

3.4.4 SaOI and ONI

On an annual basis (Fig. 3), the SaOI has a moderate and statistically significant negative correlation with (ONI) (−0.44). These finding reflects an association where El Niño phases (positive ONI) tend to weaken the Saharan pressure gradient, while La Niña phases (negative ONI) tend to strengthen it. This anticorrelation on annual timescales is an indication of a major connection between tropical Pacific variability and atmospheric dynamics of Saharan region.

Seasonally, an inverse relation appears via numerous significant correlations from late winter through summer and early autumn (Fig. 4). During the late cold season, the SaOI (JFM) manifests statistically significant correlations with ONI of JFM (−0.45), FMA (−0.45), and MAM (−0.40). The values indicate that the El Niño conditions in early spring suppress SaOI by weakening the land-sea thermal gradients that somehow interrupt the vertical circulation favorable to Saharan pressure anomalies.

The precursory teleconnection persisted and intensified throughout the summer. The JJA of SaOI is anticorrelated with ONI at various lags: JJA (−0.42), JAS (−0.43), ASO (−0.44), SON (−0.44), OND (−0.45), and even NDJ (−0.41). These correlations suggest that the influence of El Niño can

persist far beyond its active phase and continue suppressing SaO throughout the warm season. Further afield, significant correlations between SaOI of JAS and ONI of OND (−0.40) and between SaOI of SON and ONI of JAS (−0.40) also testify in favor of the teleconnection's endurance until early autumn.

The anticorrelation between SaOI and ONI reflects a likely delayed response of Saharan pressure gradients to tropical Pacific warming. El Niño events, by altering the Walker and Atlantic Hadley circulations, can reduce the land-sea thermal gradient over the Sahara, thereby weakening the Saharan Low with a seasonal lag (L'Heureux et al. 2013; Mohino et al. 2011). This teleconnection is most evident in the warm season and warrants further investigation using lagged composite analysis.

Such weakening of the Saharan Low is frequently accompanied by delayed or suppressed West African monsoon onset, leading to increased drought risk in the Sahel and Maghreb. The resulting reduction in rainfall adversely affects rain-fed agriculture, shortens growing seasons, impedes vegetation recovery, and exacerbates food insecurity across the region (Janicot et al.,1998; Sultan and Gaetani 2016; Tanarhte et al. 2024; Tefera et al. 2025).

Contrary to the typical El Niño-associated weakening of SaOI and Saharan Low, certain phases coincide with a reinforced Saharan Low and elevated land-sea thermal contrast. In spring, this amplified thermal environment, especially when compounded by dry soils and heat stress conditions documented in semi-arid regions (Alvar-Beltrán et al. 2021), can trigger early extreme heat events across North Africa and southern Europe (Lavaysse et al. 2016; Ntoumos et al. 2022).

The heatwaves resulting from these conditions exacerbate hydric stress, intensify evapotranspiration, and heighten the risk of wildfires. These degrading circumstances have immediate impacts on human health, including increased hospital admissions and mortality due to heatstroke, as well as cardiovascular and respiratory complications particularly among vulnerable populations such as the elderly and children (Kovats and Hajat 2008).

3.4.5 SaOI and other LSCIs (TNAI-TSAI-WHPI)

The seasonal correlation analysis failed to yield evidence for any statistically significant annual association between the SaOI and TNAI or TSAI. Nonetheless, a number of moderate yet statistically significant seasonal associations were identified, predominantly between late winter and summer (Fig. 4).

SaOI and TNAI-TSAI The SaOI for JFM is negatively correlated with TNAI in FMA (−0.45) and MAM (−0.43) seasons, indicating that warmer SST anomalies in the tropical North Atlantic during early spring are associated with a weakening of the Saharan pressure gradient. This relationship continues its negative trajectory in FMA and MAM, with SaOI being significantly anticorrelated to TNAI in FMA (−0.40), MAM (−0.43), AMJ (−0.40), and again in MAM with TNAI in FMA (−0.45), AMJ (−0.46), and MJJ (−0.45). Thus, a persistent teleconnection holds through spring during which positive TNAI phases likely inhibit the development of SaOI and, consequently, dust emission.

On the other hand, the TSAI-SaOI features a consistent, moderate-strength positive correlation during the warm season. From MJJ, SaOI appears positively correlated with TSAI in these intervals: MAM (0.40), AMJ (0.41), MJJ (0.41), and JJA (0.40). This interaction intensifies during JJA, whereby SaOI is positively correlated with TSAI in these seasons: JFM (0.42), FMA (0.44), MAM (0.46), AMJ (0.47), MJJ (0.46), JJA (0.46), and JAS (0.45). These interactions extend into early autumn, with SaOI in JAS correlated with TSAI in JJA (0.42), JAS (0.44), and ASO (0.42), and SaOI in ASO correlated with TSAI in JAS (0.41). These findings imply an uninterrupted warm-season influence of the southern tropical Atlantic on Saharan atmospheric dynamics.

The negative seasonal correlations with TNAI suggest that anomalously warm SSTs in the tropical North Atlantic during late winter and spring tend to suppress SaOI by weakening the Saharan thermal low and delaying the onset of regional convective activity. This mechanism can hinder the early stages of West African monsoon, increase drought risk, and disrupt rainfed agriculture in the Sahel and Maghreb (Rodríguez-Fonseca et al., 2016; Suárez-Moreno et al. 2018; Sultan and Gaetani 2016).

On the other hand, the positive correlation between TSAI and SaOI in the summer hints that warming of the tropical South Atlantic serves to strengthen the Saharan heat low by means of the land-sea thermal contrast (Gaetani et al. 2017; Imane et al. 2022). Amplified SaOI causes adverse dust-emission events and sustained dry conditions in North Africa. The accumulation of dust and extreme heat increases the probability of heatwaves and deteriorates air quality, thereby exacerbating health risks, particularly for those with respiratory and cardiovascular conditions (Chang et al. 2023; Klose 2014).

SaOI and WHPI During late winter (JFM), the SaOI exhibits a moderate negative correlation with the WHPI (−0.43), indicating that warm SSTs in the Pacific-Atlantic Warm Pool are associated with a weakening of the Saharan pressure gradient. The relationship is also evident later in the year: the JJA SaOI is negatively correlated with the OND WHPI

(−0.41), suggesting an inverse influence from the WHPI on Saharan circulation patterns across different seasons.

These inverse relationships imply that high SSTs over the western tropical Pacific and Atlantic may suppress the SaOI by modifying large-scale tropical atmospheric circulations, mainly through the weakening of the Walker and Hadley cells (Gastineau et al. 2009; Sun et al. 2022; Wang 2005). This, in turn, may delay the thermal buildup over the Sahara in winter, diminish sand dust emissions, and restrain pre-monsoonal convective activities over the Sahel.

The delayed lag in summer (SaOI in JJA and WHPI in OND) suggests that the influence of western tropical SST anomalies may persist into the warm season, modulating the Saharan Heat Low and weakening the regional pressure contrast. This eventually affects summer dust transport intensity and pathways, creating downstream effects on air quality and regional climate over the Sahel and Mediterranean margins (Suárez-Moreno et al., 2019; Sultan and Gaetani 2016; Wang et al. 2015).

To further synthesize the most influential drivers of Saharan atmospheric variability, Table 2 ranks the top 10 statistically robust seasonal teleconnections identified during the 1950–2024 period. The ranking is dominated by the coupling between the SaOI and the NAOI, particularly during the boreal winter (DJF and JFM), where correlation coefficients reach their maximum values (r=0.58 and 0.57). This significant coupling highlights the coherent behavior of North Atlantic pressure systems during the cold season. The top-ranked associations also reveal lead–lag relationships, such as the influence of DJF NAOI conditions on the subsequent JFM SaOI, suggesting a degree of atmospheric persistence. Furthermore, the inclusion of the TSAI-SaOI coupling (r=0.46) reflects a seasonal transition toward tropical Atlantic influence during the spring-to-summer period (AMJ-JJA), complemented by significant negative associations with ENSO (ONI) during summer. These results indicate that while the North Atlantic provides the primary dynamical framework for the SaOI, the dominant climatic drivers shift seasonally as the global climate system evolves through the annual cycle.

Table 2 Summary of the top 10 statistically robust seasonal teleconnections between the SaOI and LSCIS (1950–2024). Results are ranked by correlation strength (r) and include only associations satisfying the Benjamini-Hochberg False Discovery Rate (FDR) adjustment $p_{FDR} < 0.05$

SaOI Season	Climate Indicator	Target Seasonal lag	Correlation (r)	FDR-adjusted p-value
DJF	NAOI	**DJF**	0.58	0.0001
JFM	NAOI	**DJF**	0.57	0.0001
JFM	NAOI	**JFM**	0.55	0.0001
FMA	NAOI	**JFM**	0.52	0.0003
NDJ	NAOI	**NDJ**	0.52	0.0003
FMA	NAOI	**DJF**	0.49	0.0013
DJF	NAOI	**NDJ**	0.48	0.0014
FMA	NAOI	**FMA**	0.48	0.0017
JJA	TSAI	**AMJ**	0.46	0.0024
MAM	NAOI	**MAM**	0.46	0.0024

4 Conclusion

This study provides, to our knowledge, the first systematic characterization of the SaOI phase behavior and teleconnections over the full observational period (1950–2024). Through standardized phase classification and a robust seasonal lag-correlation analysis accounting for effective degrees of freedom N_{eff} and multiple testing (FDR), we documented three distinct temporal epochs and identified a pronounced regime shift toward positive-neutral phase dominance after 1990, with markedly reduced negative phase frequency post-2010. This observed non-stationarity raises fundamental questions regarding whether recent patterns reflect decadal climate variability or a structural reorganization of North Atlantic-Saharan atmospheric dynamics in response to anthropogenic forcing.

Annual and seasonal analyses reveal moderate but statistically moderate teleconnections between the SaOI and key climate drivers. After adjusting for serial correlation, the Big Three perennial indicators, the NAOI $(r = 0.42)$, AOI $(r = 0.42)$, and ONI $(r = 0.44)$, emerged as the primary drivers of SaOI variability. Seasonal lag-correlations further demonstrate that these relationships vary systematically across the annual cycle, with moderate connections coupling to the NAOI and AOI occurring from late winter through early spring. In contrast, the SaOI exhibits a persistent inverse relationship with the ONI extending from spring through autumn. Additionally, the inclusion of 13 LSCIs in this study allowed for the identification of secondary but significant seasonal associations with the TNAI, TSAI, and WHPI underscoring the SaOI's sensitivity to both tropical Atlantic SST variability and broader hemispheric forcing mechanisms.

Physically, positive SaOI phases, characterized by an intensified Azores High and deepened Saharan Thermal Low, enhance subsidence, suppress precipitation, and strengthen trade winds. These conditions amplify drought risk and dust mobilization across northwestern Africa and the Mediterranean, particularly when acting in synergy with positive NAOI/AOI phases or La Niña conditions (negative ONI). Conversely, negative SaOI phases promote moisture advection and convective activity, fostering wetter conditions specifically during winter and early spring. This configuration is often reinforced by negative NAOI/AOI phases

or El Niño events (positive ONI), which weaken the subtropical high-pressure belt and allow westerly storm tracks to penetrate the North African basin.

These findings establish the SaOI as a robust diagnostic tool for the Euro-Atlantic-African sector. The documented phase structure and identified lagged teleconnection patterns provide essential groundwork for integrating the SaOI into subseasonal-to-seasonal (S2S) prediction frameworks and early warning systems targeting drought, extreme heat mitigation, and public health preparedness (Agbehadji et al. 2023; Islam et al. 2025). Specifically, the identification of lagged relationships between the SaOI and tropical SST indices offers potential predictability at lead times relevant for agricultural planning and public health preparedness.

Future research will extend this framework through spatial correlation assessments to examine the relationships between SaOI phases and key environmental variables, including precipitation, near-surface temperature, wind fields, and aerosol optical depth (AOD) over the 1950–2024 period. Such analyses, analogous to spatial studies conducted for the NAO (Hurrell and Deser 2009) and ENSO (Ropelewski and Halpert 1989), will elucidate the geographic footprint of SaOI variability. Furthermore, applying machine learning algorithms, such as random forests or recurrent neural networks, to these spatial patterns could enable the development of hybrid dynamical-statistical forecasting systems. These tools would leverage the physical understanding of SaOI dynamics established here to improve the prediction of climate extremes and air quality degradation, supporting climate-resilient decision-making across the Sahel and Mediterranean regions.

Supplementary Information The online version contains supplementary material available at https://doi.org/10.1007/s00704-026-06305-9.

Acknowledgements The authors would like to acknowledge the support provided by the GeoHealth Hub for Climate Change and Health in the Middle East and North Africa. The GeoHealth Hub was established through Grant #5U2RTW012228 and #U01TW012237 from the National Institutes of Health (NIH) Fogarty International Center (FIC).

Author contributions Y.T. conceived the study, performed the data analysis, and wrote the initial manuscript draft. K.K. contributed to the interpretation of results and provided critical revisions. M.K. contributed to methodological validation and manuscript editing. All authors read and approved the final manuscript.

Funding This study was supported by the GeoHealth Hub for Climate Change and Health in the Middle East and North Africa (Grant #5U2RTW012228 and #U01TW012237).
Competing Interests The authors have no relevant financial or non-financial interests to disclose.

Data availability The ERA5 reanalysis dataset used in this study is publicly available from the Copernicus Climate Data Store ([https://cds.climate.copernicus.eu/](https:/cds.climate.copernicus.eu)). Proces sed SaOI data and supporting analysis scripts are available from the corresponding author upon reasonable request.

Declarations

Competing interests The authors declare no competing interests.

References

Agbehadji IE, Mabhaudhi T, Botai J, Masinde M (2023) A Systematic Review of Existing Early Warning Systems' Challenges and Opportunities in Cloud Computing Early Warning Systems. In Climate (Vol. 11, Number 9). Multidisciplinary Digital Publishing Institute (MDPI). https://doi.org/10.3390/cli11090188

Alvar-Beltrán J, Heureux A, Soldatova N, Gbangou T, Volk J (2021) Climate change and West African agriculture: case studies on adaptations and resilience. Front Sustain Food Syst 5:824806. https://doi.org/10.3389/fsufs.2021.824806

Aru H, Chen S, Chen W (2021) Comparisons of the different definitions of the Western Pacific pattern and associated winter climate anomalies in Eurasia and North America. Int J Climatol 41(4):2840–2859. https://doi.org/10.1002/joc.6993

Barnston AG, Livezey RE (1987) Classification, seasonality and persistence of low-frequency atmospheric circulation patterns. Mon Weather Rev 115(6):1083–1126.

Benjamini Y, Hochberg Y (1995) Controlling the false discovery rate: a practical and powerful approach to multiple testing. J Roy Stat Soc B 57(1):289–300. https://doi.org/10.1111/j.2517-6161.1995.tb02031.x

Boer GJ, Sospedra-Alfonso R (2019) Assessing the skill of the Pacific Decadal Oscillation (PDO) in a decadal prediction experiment. Clim Dyn. https://doi.org/10.1007/s00382-019-04896-w

Bouguerra H, Derdous O, Tachi SE, Hatzaki M, Abida H (2024) Spatiotemporal investigation of meteorological drought variability over northern Algeria and its relationship with different atmospheric circulation patterns. Theoret Appl Climatol 155(2):1507–1518. https://doi.org/10.1007/s00704-023-04705-9

Chang JH, Lee YL, Chang LT, Chang TY, Hsiao TC, Chung KF, Ho KF, Kuo HP, Lee KY, Chuang KJ, Chuang HC (2023) Climate change, air quality, and respiratory health: a focus on particle deposition in the lungs. Ann Med. https://doi.org/10.1080/07853890.2023.2264881

CHEN SF, WU R (2017) An enhanced influence of sea surface temperature in the tropical northern Atlantic on the following winter ENSO since the early 1980s. Atmospheric Ocean Sci Lett 10(2). https://doi.org/10.1080/16742834.2016.1259542

Clement A, DiNezio P, Deser C (2011) Rethinking the ocean's role in the Southern Oscillation. J Clim 24(15). https://doi.org/10.1175/2011JCLI3973.1

Cramer W, Guiot J, Fader M, Garrabou J, Gattuso JP, Iglesias A, Lange MA, Lionello P, Llasat MC, Paz S, Peñuelas J, Snoussi M, Toreti A, Tsimplis MN, Xoplaki E (2018) Climate change and interconnected risks to sustainable development in the Mediterranean. Nat Clim Chang 8(11):972–980. https://doi.org/10.1038/s41558-018-0299-2

Criado-Aldeanueva F, Soto-Navarro J (2020) Climatic indices over the Mediterranean Sea: A review. Appl Sci 10(17):5790. https://doi.org/10.3390/app10175790

Davis RE, Hayden BP, Gay DA, Phillips WL, Jones GV (1997) The North Atlantic subtropical anticyclone. J Clim 10(4):728–744.

Deser C, Trenberth K, Staff N (2016) The Climate Data Guide: Pacific Decadal Oscillation (PDO): Definition and Indices. National Center for Atmospheric Research. [Online Resource] Available at: https://climatedataguide.ucar.edu/climate-data/pacific-decadal-oscillation-pdo-definition-and-indices (Accessed March 2026)

Dosio A, Jones RG, Jack C, Lennard C, Nikulin G, Hewitson B (2019) What can we know about future precipitation in Africa? Robustness, significance and added value of projections from a large ensemble of regional climate models. Clim Dyn 53(9–10):5833–5858. https://doi.org/10.1007/s00382-019-04900-3

Dosio A, Turner AG, Tamoffo AT, Sylla MB, Lennard C, Jones RG, Terray L, Nikulin G, Hewitson B (2020) A tale of two futures: Contrasting scenarios of future precipitation for West Africa from an ensemble of regional climate models. Environ Res Lett 15(6). https://doi.org/10.1088/1748-9326/ab7fde

Enfield DB, Lee SK, Wang C (2006) How are large Western Hemisphere warm pools formed? Prog Oceanogr 70:2–4. https://doi.org/10.1016/j.pocean.2005.07.006

Enfield DB, Mestas-Nuñez AM, Trimble PJ (2001) The Atlantic multidecadal oscillation and its relation to rainfall and river flows in the continental U.S. Geophys Res Lett 28(10):2077–2080. https://doi.org/10.1029/2000GL012745

Fang Z, Sun X, Yang XQ, Zhu Z (2024) Interdecadal Variations in the Spatial Pattern of the Arctic Oscillation Arctic Center in Wintertime. Geophys Res Lett 51(22). https://doi.org/10.1029/2024GL111380

Fogt RL, Marshall GJ (2020) The Southern Annular Mode: Variability, trends, and climate impacts across the Southern Hemisphere. In Wiley Interdisciplinary Reviews: Climate Change (Vol. 11, Number 4). Wiley-Blackwell. https://doi.org/10.1002/wcc.652

Frankcombe LM, von der Heydt A, Dijkstra HA (2010) North Atlantic multidecadal climate variability: an investigation of dominant time scales and processes. J Clim 23(13):3626–3638. https://doi.org/10.1175/2010JCLI3471.1

Frierson DMW, Lu J, Chen G (2007b) Width of the Hadley cell in simple and comprehensive general circulation models. Geophys Res Lett 34(18). https://doi.org/10.1029/2007GL031115

Frierson, D. M. W., Lu, J., & Chen, G. (2007). Width of the Hadley cell in simple and comprehensive general circulation models. Geophysical Research Letters, 34(18), L18804 https://doi.org/10.1029/2007GL031115

Gaetani M, Flamant C, Bastin S, Janicot S, Lavaysse C, Hourdin F, Braconnot P, Bony S (2017) West African monsoon dynamics and precipitation: the competition between global SST warming and CO2 increase in CMIP5 idealized simulations. Clim Dyn 48(3–4):1353–1373. https://doi.org/10.1007/s00382-016-3146-z

Gastineau G, Li L, Le Treut H (2009) The Hadley and Walker circulation changes in global warming conditions described by idealized atmospheric simulations. J Clim 22(14):3993–4013. https://doi.org/10.1175/2009JCLI2794.1

Gershunov A, Barnett TP (1998) Interdecadal modulation of ENSO teleconnections. Bull Am Meteorol Soc 79(12):2715–2725.

Giannini A, Saravanan R, Chang P (2003) Oceanic forcing of Sahel rainfall on interannual to interdecadal time scales. Science 302(5647):1027–1030. https://doi.org/10.1126/science.1089357

Glantz MH, Ramirez IJ (2020) Reviewing the Oceanic Niño Index (ONI) to enhance societal readiness for El Niño's impacts. Int J Disaster Risk Sci 11(3):394–403. https://doi.org/10.1007/s13753-020-00275-w

Goudie AS, Middleton NJ (2001) Saharan dust storms: nature and consequences. Earth Sci Rev 56(1–4):179–204. https://doi.org/10.1016/S0012-8252(01)00067-8

Hersbach H, Bell B, Berrisford P, et al. (2020). The ERA5 global reanalysis. Q J R Meteorol Soc 146(730):1999–2049. https://doi.org/10.1002/qj.3803

Hurrell JW (1995) Decadal trends in the North Atlantic Oscillation. Science (New York, N.Y.) 269:676–679. https://doi.org/10.1126/science.269.5224.676

Hurrell JW, Deser C (2009) North Atlantic climate variability: The role of the North. https://doi.org/10.1016/j.marsys.2008.11.026. Atlantic Oscillation ☆

Hurrell JW, Kushnir Y, Ottersen G, Visbeck M (2003) An overview of the north atlantic oscillation. In Geophysical Monograph Series (Vol. 134, pp. 1–35). Blackwell Publishing Ltd. https://doi.org/10.1029/134GM01

Hu S, Zhang W, Jin FF, Hong LC, Jiang F, Stuecker MF (2023) Seasonal dependence of the Pacific-North American Teleconnection associated with ENSO and its interaction with the annual cycle. J Clim 36(20):7061–7072. https://doi.org/10.1175/JCLI-D-23-0148.1

Imane S, Oumaima B, Kenza K, Laila I, Youssef E, Zineb S, Mohamed E (2022) A review on climate, air pollution, and health in North Africa. Curr Environ Health Rep 9(2):276–298. https://doi.org/10.1007/s40572-022-00350-y

Islam MM, Hasan M, Mia MS, Masud A, A., Islam ARMT (2025) Early warning systems in climate risk management: Roles and implementations in eradicating barriers and overcoming challenges. https://doi.org/10.1016/j.nhres.2025.01.007. Natural Haz ards Research (in press)

Janicot S, Harzallah A, Fontaine B, Moron V (1998) West African monsoon dynamics and eastern equatorial Atlantic and Pacific SST anomalies (1970-88). J Clim 11(8):1874–1882.

Jones PD, Jonsson T, Wheeler D (1997) Extension to the North Atlantic Oscillation using early instrumental pressure observations from Gibraltar and south-west Iceland. Int J Climatol 17(13):1433–1450.

Khomsi K, Bouakline O, Sekmoudi I (2024) A review of large-scale climate indicators (LSCI) and their environmental and health implications in the Mediterranean region. Air Qual Atmos Health 17(3):581–597. https://doi.org/10.1007/s11869-023-01465-3

Khomsi K, Najmi H, Chelhaoui Y, Souhaili Z (2020) The contribution of large-scale atmospheric patterns to PM10 pollution: The new Saharan oscillation index. Aerosol Air Qual Res 20(5):1038–1047. https://doi.org/10.4209/aaqr.2019.08.0401

Klose MR (2014) Convective turbulent dust emission: Process, parameterization, and relevance in the Earth system [Doctoral dissertation, University of Cologne]. https://kups.ub.uni-koeln.de/5778/

Kovats RS, Hajat S (2008) Heat stress and public health: A critical review. Annu Rev Public Health 29:41–55. https://doi.org/10.1146/annurev.publhealth.29.020907.090843

Lavaysse C, Cammalleri C, Dosio A, Van Der Schrier G, Toreti A, Vogt J (2018) Towards a monitoring system of temperature extremes in Europe. Nat Hazards Earth Syst Sci 18(1):91–104. https://doi.org/10.5194/nhess-18-91-2018

Lavaysse C, Flamant C, Evan A, Janicot S, Gaetani M (2016) Recent climatological trend of the Saharan heat low and its impact on the West African climate. Clim Dyn 47(11):3479–3498. https://doi.org/10.1007/s00382-015-2847-z

Lee AFS, Heghinian SM (1977) A shift of the mean level in a sequence of independent normal random variables a Bayesian approach. Technometrics 19(4):503–506. https://doi.org/10.1080/00401706.1977.10489592

Lelieveld J, Barlas C, Giannadaki D, Pozzer A (2013) Model calculated global, regional and megacity premature mortality due to air pollution. Atmos Chem Phys 13(14):7023–7037. https://doi.org/10.5194/acp-13-7023-2013

Lelieveld J, Evans JS, Fnais M, Giannadaki D, Pozzer A (2015) The contribution of outdoor air pollution sources to premature mortality on a global scale. Nature 525(7569):367–371. https://doi.org/10.1038/nature15371

L'Heureux ML, Lee S, Lyon B (2013) Recent multidecadal strengthening of the Walker circulation across the tropical Pacific. Nat Clim Change 3(6):571–576. https://doi.org/10.1038/nclimate1840

LiJ, Wang JXL (2003) A new North Atlantic Oscillation index and its variability. Adv Atmos Sci 20(5):661–676. https://doi.org/10.1007/BF02915394

Li J, Wang JXL (2003) A new North Atlantic Oscillation index and its variability. Adv Atmos Sci 20(5):661–676. https://doi.org/10.1007/bf02915394

Li R, Wang SY, Gillies RR, Buckley BM, Truong LH, Cho C (2015) Decadal oscillation of autumn precipitation in Central Vietnam modulated by the East Pacific-North Pacific (EP-NP) teleconnection. Environ Res Lett. https://doi.org/10.1088/1748-9326/10/2/024008

López-Magaña J, Hurtado-Oliva MÁ, Guzón-Zatarain O, Manzano-Sarabia M (2022) Interannual Spatial Variability of the Western Hemisphere Warm Pool and the Impacts on Marine Protected Areas in the Mexican Pacific. J Coastal Res 38(2). https://doi.org/10.2112/JCOASTRES-D-21-00049.1

López-Moreno JI, Vicente-Serrano SM (2008) Positive and negative phases of the wintertime North Atlantic Oscillation and drought occurrence over Europe: A multitemporal-scale approach. J Clim 21(6). https://doi.org/10.1175/2007JCLI1739.1

Luppichini M, Lazzarotti M, Bini M (2024) Climate change as main driver of centennial decline in river sediment transport across the Mediterranean region. J Hydrol 636. https://doi.org/10.1016/j.jhydrol.2024.131266

Lu,Z., Zhang, Q., Miller, P. A., Zhang, Q., Berntell, E., & Smith, B. (2021). Impacts of large-scale Sahara solar farms on global climate and vegetation. Geophysical Research Letters, 48(2), e2020GL090789 https://doi.org/10.1029/2020GL090789

Mantua NJ, Hare SR, Zhang Y, Wallace JM, Francis RC (1997) A Pacific interdecadal climate oscillation with impacts on salmon production. Bull Am Meteorol Soc 78(6):1069–1079.

Mazouz R, Assani AA, Rodríguez MA (2013) Application of redundancy analysis to hydroclimatology: a case study of spring heavy floods in southern Québec (Canada). J Hydrol. https://doi.org/10.1016/j.jhydrol.2013.05.035

Meehl GA, Hu A, Teng H (2016) Initialized decadal prediction for transition to positive phase of the Interdecadal Pacific Oscillation. Nat Commun. https://doi.org/10.1038/ncomms11718

Middleton NJ (1985) Effect of drought on dust production in the Sahel. Nature 316(6027):431–434. https://doi.org/10.1038/316431a0

Minobe S, Mantua N (1999) Interdecadal modulation of interannual atmospheric and oceanic variability over the North Pacific. Prog Oceanogr 43(2–4):163–192. https://doi.org/10.1016/S0079-6611(99)00008-5

Mohino E, Rodríguez-Fonseca B, Mechoso CR, Gervois S, Ruti P, Chauvin F (2011) Impacts of the tropical Pacific/Indian oceans on the seasonal cycle of the West African monsoon. J Clim 24(15):3878–3891. https://doi.org/10.1175/2011JCLI3988.1

Nicholson SE (2013) The West African Sahel: a review of recent studies on the rainfall regime and its interannual variability. ISRN Meteorol 2013:1–32. https://doi.org/10.1155/2013/453521

Ntoumos A, Hadjinicolaou P, Zittis G, Proestos Y, Lelieveld J (2022) Projected air temperature extremes and maximum heat conditions over the Middle-East-North Africa (MENA) region. Earth Syst Environ 6(2):343–359. https://doi.org/10.1007/s41748-022-00297-y

Palutikof JP (2003) Analysis of Mediterranean Climate Data: Measured and Modelled. In Springer-Verlag (pp. 125–132). https://doi.org/10.1007/978-3-642-55657-9_6

Park JH, Kug JS, Li T, Behera SK (2018) Predicting El Niño beyond 1-year lead: effect of the Western Hemisphere Warm Pool. Sci Rep. https://doi.org/10.1038/s41598-018-33191-7

Paz S, Tourre YM, Planton S (2003) North Africa-West Asia (NAWA) sea-level pressure patterns and their linkages with the Eastern Mediterranean (EM) climate. Geophys Res Lett 30(19). https://doi.org/10.1029/2003GL017862

Perkins-Kirkpatrick SE, Lewis SC (2020) Increasing trends in regional heatwaves. Nat Commun 11(1). https://doi.org/10.1038/s41467-020-16970-7

Pettitt AN (1979) A Non-Parametric Approach to the Change-Point Problem. In Source: Journal of the Royal Statistical Society. Series C (Applied Statistics) (Vol. 28, Number 2)

Pokorná L, Huth R (2015) Climate impacts of the NAO are sensitive to how the NAO is defined. Theor Appl Climatol 119(3–4):639–652. https://doi.org/10.1007/s00704-014-1116-0

Power SB, Kociuba G (2011) The impact of global warming on the Southern Oscillation Index. Clim Dyn 37(9–10):1745–1754. https://doi.org/10.1007/s00382-010-0951-7

Prospero JM, Ginoux P, Torres O, Nicholson SE, Gill TE (2002) Environmental characterization of global sources of atmospheric soil dust identified with the Nimbus 7 Total Ozone Mapping Spectrometer (TOMS) absorbing aerosol product. Rev Geophys 40(1):2-1–2-31. https://doi.org/10.1029/2000RG000095

Pu B, Ginoux P (2017) Projection of American dustiness in the late 21st century due to climate change. Sci Rep. https://doi.org/10.1038/s41598-017-05431-9

Pyper BJ, Peterman RM (1998) Comparison of methods to account for autocorrelation in correlation analyses of fish data. Can J Fish Aquat Sci 55(9):2127–2140. https://doi.org/10.1139/f98-104

Rodríguez-Fonseca B, Polo I, García-Serrano J, Losada T, Mohino E, Mechoso CR, Kucharski F (2009) Are Atlantic Niños enhancing Pacific ENSO events in recent decades? Geophys Res Lett 36(20). https://doi.org/10.1029/2009GL040048

Rodríguez-Fonseca B, Suárez-Moreno R, Ayarzagüena B, López-Parages J, Gómara I, Villamayor J, Mohino E, Losada T, Castaño-Tierno A (2016a) A review of ENSO influence on the North Atlantic. A non-stationary signal. In Atmosphere (Vol. 7, Number 7). MDPI AG. https://doi.org/10.3390/atmos7070087

Ropelewski CF, Halpert MS (1989) Precipitation patterns associated with the high index phase of the Southern Oscillation. J Clim 2(3):268.

Santer BD, Wigley TML, Boyle JS, Gaffen DJ, Hnilo JJ, Nychka D, Parker DE, Taylor KE (2000) Statistical significance of trends and trend differences in layer-average atmospheric temperature time series. J Geophys Res Atmos 105(D6):7337–7356. https://doi.org/10.1029/1999JD901105

Schwing FB, Murphree T, Green PM (2002) The Northern Oscillation Index (NOI): A new climate index for the northeast Pacific. In Progress in Oceanography (Vol. 53, Numbers 2–4). https://doi.org/10.1016/S0079-6611(02)00027-7

Sebbar A et al (2011) Étude des variations climatiques de la région centre du Maroc, vol 24. Publications de l'Association Internationale de Climatologie, pp 321–326

Sheng C, Zhang S, Liu Y, Wu G, He B (2023) Interannual impact of tropical southern Atlantic SST on surface air temperature over East Asia during boreal spring. Npj Clim Atmospheric Sci 6(1). https://doi.org/10.1038/s41612-023-00515-y

Sultan B, Gaetani M (2016) Agriculture in West Africa in the twenty-first century: climate change and impacts scenarios, and potential for adaptation. Front Plant Sci. https://doi.org/10.3389/fpls.2016.01262

Sun C, Liu Y, Wei T, Kucharski F, Li J, Wang C (2022) Cross-hemispheric SST propagation enhances the predictability of tropical western Pacific climate. Npj Clim Atmospheric Sci 5(1). https://doi.org/10.1038/s41612-022-00262-6

Suárez-Moreno R, Rodríguez-Fonseca B, Barroso JA, Fink AH (2018) Interdecadal changes in the leading ocean forcing of Sahelian rainfall interannual variability: atmospheric dynamics and role of multidecadal SST background. J Clim 31(17):6687–6710. https://doi.org/10.1175/JCLI-D-17-0367.1

Suárez-Moreno, R., Rodríguez-Fonseca, B., & Encinas, L. H. (2019). The Saharan Heat Low and its modulation by tropical Atlantic and Pacific SSTs. Climate Dynamics, 53(1-2), 1-18 https://doi.org/10.1007/s00382-018-4566-

Tanarhte M, De Vries AJ, Zittis G, Chfadi T (2024) Severe droughts in North Africa: a review of drivers, impacts and management. Earth-Sci Rev. https://doi.org/10.1016/j.earscirev.2024.104701

Tefera ML, Seddaiu G, Carletti A, Awada H (2025) Rainfall variability and drought in West Africa: challenges and implications for rain-fed agriculture. Theoret Appl Climatol 156 (in press. https://doi.org/10.1007/s00704-024-05251-8

ThompsonDWJ, Wallace JM (1998) The Arctic Oscillation signature in the wintertime geopotential height and temperature fields. Geophys Res Lett 25(9):1297–1300. https://doi.org/10.1029/98GL00950

Thompson DWJ, Wallace JM (2001) Regional climate impacts of the Northern Hemisphere annular mode. Science 293(5527):85–89. https://doi.org/10.1126/science.1058958

Tourre YM, Paz S, Cassou C, Kutiel H (2006) Atmospheric dynamics over northwest Africa and linkages with Sahelian rainfall. Geophys Res Lett 33(14). https://doi.org/10.1029/2006GL026695

Trenberth KE (1997) The definition of El Niño. Bull Am Meteorol Soc 78(12):2771–2777.

Verner D, Tréguer D, Redwood J, Christensen J, McDonnell R, Elbert C, Konishi Y, Belghazi S (2018) Climate variability, drought, and drought management in Morocco's agricultural sector. World Bank Group, Washington DC. https://doi.org/10.1596/29662

VimontI, Deser C, Alexander MA (2022) The role of the seasonal cycle in the Pacific-North American teleconnection response to ENSO. J Clim 35(11):3321–3341. https://doi.org/10.1175/JCLI-D-21-0678.1

Vitart F, Ardilouze C, Bonet A, Brookshaw A, Chen M, Codorean C, Déqué M, Ferranti L, Fucile E, Fuentes M, Hendon H, Hodgson J, Kang HS, Kumar A, Lin H, Liu G, Liu X, Malguzzi P, Mallas I, Zhang L (2017) The subseasonal to seasonal (S2S) prediction project database. Bull Am Meteorol Soc 98(1):163–173. https://doi.org/10.1175/BAMS-D-16-0017.1

WallaceJM, Gutzler DS (1981) Teleconnections in the geopotential height field during the Northern Hemisphere winter. Mon Weather Rev 109(4):784–812. https://journals.ametsoc.org/view/journals/mwre/109/4/1520-0493_1981_109_0784_titgfh_2_0_co_2.xml

Wang C (2005) ENSO, Atlantic climate variability, and the Walker and Hadley circulations. In R. S. Bradley & J. D. Diaz (Eds.), The Hadley Circulation: Present, Past and Future (pp. 173–202). Springer. https://doi.org/10.1007/978-1-4020-2944-8_7

Wang C, Enfield DB (2001) The tropical Western Hemisphere warm pool. Geophys Res Lett 28(8):1635–1638. https://doi.org/10.1029/2000GL011763

Wang W, Evan AT, Flamant C, Lavaysse C (2015) On the decadal scale correlation between African dust and Sahel rainfall: the role of Saharan heat low-forced winds. Sci Adv 1(9):e1500646. https://doi.org/10.1126/sciadv.1500646

Xiao D, Ren HL (2023) A regime shift in North Pacific annual mean sea surface temperature in 2013/14. Front Earth Sci. https://doi.org/10.3389/feart.2022.987349

Yang Q, Fan L (2023) On the Decadal Changes of the Interannual Relationship Between ENSO and Tropical South Atlantic SST in Boreal Summer. Geophys Res Lett 50(18). https://doi.org/10.1029/2023GL104355

ZhugeA, Tan B (2018) The springtime Western Pacific pattern: its formation and maintenance mechanisms and climate impacts. J Clim 31(17):7229–7250. https://doi.org/10.1175/JCLI-D-18-0153.1

Zhuge A, Tan B (2021) The springtime Western Pacific pattern: its formation and maintenance mechanisms and climate impacts. J Clim 34(17):7229–7250. https://doi.org/10.1175/JCLI-D-20-0500.1

Publisher's note Springer Nature remains neutral with regard to jurisdictional claims in published maps and institutional affiliations.

Springer Nature or its licensor (e.g. a society or other partner) holds exclusive rights to this article under a publishing agreement with the author(s) or other rightsholder(s); author self-archiving of the accepted manuscript version of this article is solely governed by the terms of such publishing agreement and applicable law.